Published by Institute of Physics Publishing for SISSA/ISAS
Received: *July 26, 2002*
Accepted: *August 1, 2002*

Radiative τ decay and the magnetic moment of the muon*

Vincenzo Cirigliano
Departament de Física Teòrica, IFIC, Universitat de València - CSIC
Apt. Correus 2085, E-46071 València, Spain
E-mail: Vincenzo.Cirigliano@ific.uv.es

Gerhard Ecker and Helmut Neufeld
Institut für Theoretische Physik, Universität Wien
Boltzmanngasse 5, A-1090 Vienna, Austria
E-mail: ecker@thp.univie.ac.at, neufeld@thp.univie.ac.at

Abstract: We discuss the decay $\tau^- \to \nu_\tau \pi^- \pi^0 \gamma$ in terms of a model with the correct low-energy structure and with the relevant resonance degrees of freedom. The nontrivial radiative dynamics becomes visible for large photon momenta only. We use the model to calculate electromagnetic corrections for the two-pion contribution to hadronic vacuum polarization extracted from photon-inclusive two-pion decays. The corrections are insensitive to the details of the model and depend on the pion form factor only. Putting all relevant isospin violating corrections together, we obtain a shift $\Delta a_\mu = (-120 \pm 26 \pm 3) \times 10^{-11}$ to be applied to determinations of the anomalous magnetic moment of the muon from photon-inclusive τ data.

Keywords: Weak Decays, Electromagnetic Processes and Properties, Chiral Lagrangians.

*Work supported in part by TMR, EC-Contract No. ERBFMRX-CT980169 (EURODAΦNE).

Contents

1. Introduction

The process $\tau^- \to \nu_\tau \pi^- \pi^0 \gamma$ involves an interplay of strong, weak and electromagnetic effects. For small momentum transfer to the hadronic system as in the related radiative pionic beta decay $\pi^+ \to e^+ \nu_e \pi^0 \gamma$, the theoretical determination of the associated decay amplitude is well under control.

At low energies, the standard model of strong and electroweak interactions is described by an effective quantum field theory called chiral perturbation theory (CHPT) [1]. It treats the interactions of the experimentally observed hadronic degrees of freedom at low energies by exploiting the constraints imposed by the symmetries of the standard model, in particular the spontaneously broken chiral symmetry. The application of CHPT is not restricted to purely strong interaction processes. With appropriate external source terms, also semileptonic and electromagnetic reactions involving leptons can be investigated.

The applicability of CHPT ends once typical hadronic energies are approaching the mass of the ρ resonance. Nevertheless, the correct low-energy limit, unambiguously described by CHPT, puts constraints on the behaviour of amplitudes also in the resonance region. The low-energy constants (LECs) of order p^4 in the chiral expansion are known to be dominated by the low-lying meson resonances [2]. This correspondence facilitates the matching between the low-energy domain and the resonance region. Applications along these lines comprise the pion form factor [3, 4], radiative ρ decays [5] and four-pion production [6].

JHEP08(2002)002

The radiative τ decay is a further process where the resonance regime of the standard model can be tested. A second motivation for the present investigation lies in the relevance of the non-radiative decay $\tau^- \to \nu_\tau \pi^- \pi^0$ for a precise determination of hadronic vacuum polarization, which is essential for the calculation of both the energy dependence of the QED fine structure constant and of the anomalous magnetic moment of the muon. The reason is that a CVC relation between electromagnetic and weak form factors allows to relate the differential decay rate of $\tau^- \to \nu_\tau \pi^- \pi^0$ to the cross section $\sigma(e^+e^- \to \pi^+\pi^-)$ in the isospin limit.

However, the present theoretical and experimental accuracy of hadronic vacuum polarization requires a precise determination of all isospin breaking effects due to $m_u \neq m_d$ and electromagnetism. The radiative corrections for $\tau^- \to \nu_\tau \pi^- \pi^0$ are part of this task. To cancel the infrared divergences generated by the one-loop exchange of a virtual photon, the associated radiative decay mode must be included.

In the low-energy limit, the necessary modifications of the CHPT framework in the presence of virtual photons [7, 8] and virtual leptons [9] have already been worked out. In this paper we want to cover also the resonance region relevant for the two-pion decay of the τ lepton. Our present work is an extension of a previous letter [10] where electromagnetic corrections and their impact on the determination of a_μ had already been discussed. However, the analysis of ref. [10] carried a rather large uncertainty because of the incomplete matching between virtual and real photons that depends on the experimental setup. In the present paper, we discuss in detail the radiative corrections for the case where all radiative events are included in the two-pion data sample. This is a case of immediate practical interest because it corresponds to the analysis of the ALEPH experiment [11].[1]

The paper is organized as follows. In section 2 we discuss the general structure of the $\tau^- \to \nu_\tau \pi^- \pi^0 \gamma$ amplitude together with the dominant contributions in the resonance region. The decay rate is calculated in section 3. Applying different cuts in the photon energy, we explore the energy region where deviations from bremsstrahlung can be expected. In section 4 we turn to the calculation of radiative corrections for the τ decay into two pions relevant for hadronic vacuum polarization. The isospin violating corrections for a_μ are collected in section 5. Finally, our conclusions are summarized in section 6. The chiral resonance lagrangian, kinematical details and loop functions are relegated to two appendices.

2. Amplitude for $\tau^- \to \nu_\tau \pi^- \pi^0 \gamma$

The matrix element for the decay

$$\tau^-(P) \to \nu_\tau(q)\pi^-(p_-)\pi^0(p_0)\gamma(k)$$

has the general structure

$$\begin{aligned} T = eG_F V_{ud}^* \varepsilon^\mu(k)^* \Big\{ & F_\nu \overline{u}(q)\gamma^\nu(1-\gamma_5)(m_\tau + \not{P} - \not{k})\gamma_\mu u(P) + \\ & + (V_{\mu\nu} - A_{\mu\nu})\overline{u}(q)\gamma^\nu(1-\gamma_5)u(P) \Big\} . \end{aligned} \qquad (2.1)$$

[1] We are grateful to Michel Davier and Andreas Höcker for information on the ALEPH procedure.

The first part of this matrix element describes bremsstrahlung off the initial τ lepton with

$$F_\nu = (p_0 - p_-)_\nu f_+(t)/2P \cdot k\,, \qquad t = (p_- + p_0)^2\,. \tag{2.2}$$

The form factor $f_+(t)$ governs the non-radiative decay. It is identical to the electromagnetic form factor of the pion because we work in the isospin limit $m_u = m_d$.

The second part of eq. (2.1) describes the vector and axial-vector components of the transition

$$W^-(P-q) \to \pi^-(p_-)\pi^0(p_0)\gamma(k)\,.$$

The hadronic tensor $V_{\mu\nu}$ contains bremsstrahlung off the π^- in the final state. Gauge invariance implies the Ward identities

$$\begin{aligned} k^\mu V_{\mu\nu} &= (p_- - p_0)_\nu f_+(t) \\ k^\mu A_{\mu\nu} &= 0\,. \end{aligned} \tag{2.3}$$

The tensor amplitudes $V_{\mu\nu}, A_{\mu\nu}$ contain four invariant amplitudes each [12]. For $V_{\mu\nu}$ we use a rather special form here that is convenient for our purposes. In $A_{\mu\nu}$ we only include the two amplitudes that actually arise in our calculation:

$$\begin{aligned} V_{\mu\nu} &= f_+\left[(P-q)^2\right]\frac{p_{-\mu}}{p_-\cdot k}(p_- + k - p_0)_\nu - f_+\left[(P-q)^2\right] g_{\mu\nu} + \\ &\quad + \frac{f_+[(P-q)^2] - f_+(t)}{(p_- + p_0)\cdot k}(p_- + p_0)_\mu (p_0 - p_-)_\nu + \\ &\quad + v_1(g_{\mu\nu} p_-\cdot k - p_{-\mu}k_\nu) + v_2(g_{\mu\nu}p_0\cdot k - p_{0\mu}k_\nu) + \\ &\quad + v_3(p_{-\mu}p_0\cdot k - p_{0\mu}p_-\cdot k)p_{-\nu} + v_4(p_{-\mu}p_0\cdot k - p_{0\mu}p_-\cdot k)(p_- + p_0 + k)_\nu \end{aligned} \tag{2.4}$$

$$A_{\mu\nu} = i a_1 \varepsilon_{\mu\nu\rho\sigma}(p_0 - p_-)^\rho k^\sigma + i a_2 (P-q)_\nu \varepsilon_{\mu\rho\sigma\tau} k^\rho p_-^\sigma p_0^\tau\,. \tag{2.5}$$

These tensor amplitudes have the following properties:

- $V_{\mu\nu}$ and $A_{\mu\nu}$ satisfy the Ward identities (2.3) for any $v_1, \ldots, v_4, a_1, a_2$.
- Taking into account $(P-q)^2 = t + 2(p_- + p_0)\cdot k$, Low's theorem [13] is manifestly satisfied:

$$\begin{aligned} V_{\mu\nu} &= f_+(t)\frac{p_{-\mu}}{p_-\cdot k}(p_- - p_0)_\nu + \\ &\quad + f_+(t)\left(\frac{p_{-\mu}k_\nu}{p_-\cdot k} - g_{\mu\nu}\right) + \\ &\quad + 2\frac{df_+(t)}{dt}\left(\frac{p_{-\mu}p_0\cdot k}{p_-\cdot k} - p_{0\mu}\right)(p_- - p_0)_\nu + O(k)\,. \end{aligned} \tag{2.6}$$

The invariant amplitudes $v_1, \ldots, v_4$ as well as a_1, a_2 remain finite for $k \to 0$. Of course, initial state bremsstrahlung in eqs. (2.1), (2.2) contributes also in the Low limit.

- The leading order in the low-energy expansion corresponds to

$$\begin{aligned} f_+ &= 1 \\ v_1 &= v_2 = v_3 = v_4 = 0 \\ a_1 &= a_2 = 0\,. \end{aligned} \tag{2.7}$$

Our aim is to construct a model for radiative τ decay that can be trusted in all of phase space. A major constraint is the correct low-energy limit to $O(p^4)$. The local contribution of $O(p^4)$ contains information on which meson resonances must be taken into account for extending the chiral amplitude into the resonance region. On the other hand, except for the pion form factor $f_+(t)$, we are not going to include all one-loop contributions arising at $O(p^4)$, let alone higher orders. Since we want to use the model for all energies accessible in τ decay a complete one-loop calculation would not be of much help anyway. Part of the loop contributions will be contained in the energy-dependent widths of the resonance propagators and in the representation of the pion form factor of ref. [3] that we shall use. Therefore, our approach uses the low-energy limit to identify the relevant degrees of freedom but the model goes clearly beyond the range of applicability of the low-energy expansion of QCD. Such a procedure works very well for the pion form factor itself [3, 4] and it also seems to be successful in radiative ρ decays [5] and in four-pion production [6].

In addition to the one-loop amplitude, $V_{\mu\nu}$ depends to $O(p^4)$ on the LECs L_9, L_{10} [1]:

$$\begin{aligned} f_+(t) &= 1 + \frac{2L_9 t}{F_\pi^2} \\ v_1 &= 4\frac{(2L_9 + L_{10})}{F_\pi^2} \\ v_2 &= 4\frac{L_{10}}{F_\pi^2} \\ v_3 = v_4 &= 0\,. \end{aligned} \tag{2.8}$$

The constants L_9, L_{10} can be interpreted as low-energy remnants of ρ and a_1 exchange [2]. As usual, ρ exchange will turn out to dominate by far and the a_1 contribution is in practice undetectable in this decay.

For completeness, we include also the (leading) contributions of $O(p^4)$ to $A_{\mu\nu}$ due to the chiral anomaly. The diagrams in figure 1 get contributions from the Wess-Zumino-Witten functional [14]:

$$a_1 = \frac{1}{8\pi^2 F_\pi^2}\,, \qquad a_2 = -\frac{1}{4\pi^2 F_\pi^2[(P-q)^2 - M_\pi^2]}\,. \tag{2.9}$$

By itself, the anomaly contribution cannot be expected to yield a realistic axial amplitude for all available energies. We take it rather as an indication of the expected order of magnitude of $A_{\mu\nu}$. Anticipating the result of the numerical calculation, the anomalous amplitude is very much suppressed compared to the dominant ρ exchange contributions and turns out to be completely negligible in radiative τ decay.

JHEP08(2002)002

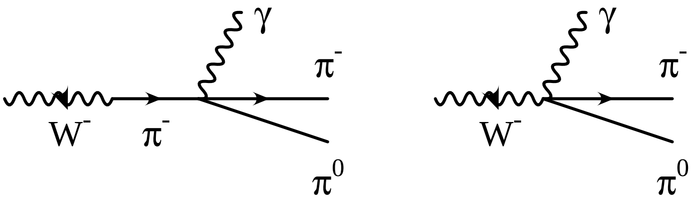

Figure 1: Anomalous diagrams for the transition $W^- \to \pi^-\pi^0\gamma$ contributing to the axial tensor amplitude $A_{\mu\nu}$.

The amplitude of $O(p^4)$ in (2.8) tells us that ρ and a_1 exchange contribute to the vector amplitude at low energies. We now assume that these are the dominant degrees of freedom for all accessible energies. As is easy to understand from the decay rates involved, a_1 exchange will be much suppressed compared to ρ exchange except at very low energies. Nevertheless, we include the a_1 contributions to $V_{\mu\nu}$.

The resonance lagrangian [2] and corresponding diagrams are displayed in appendix A. The lagrangian gives also rise to double-ρ exchange diagrams. One of them is needed for ensuring gauge invariance beyond $O(p^4)$ accuracy but we include all of them for consistency. In terms of the couplings defined in appendix A, the final result takes the form:

$$
\begin{aligned}
v_1 &= \frac{F_V G_V}{F_\pi^2 M_\rho^2}\left\{2 + 2M_\rho^2 D_\rho^{-1}\left[(P-q)^2\right] + tD_\rho^{-1}(t) + tM_\rho^2 D_\rho^{-1}(t) D_\rho^{-1}\left[(P-q)^2\right]\right\} + \\
&\quad + \frac{F_V^2}{2F_\pi^2 M_\rho^2}\left\{-1 - M_\rho^2 D_\rho^{-1}\left[(P-q)^2\right] + (P-q)^2 D_\rho^{-1}\left[(P-q)^2\right]\right\} + \\
&\quad + \frac{F_A^2}{F_\pi^2 M_{a_1}^2}\left(M_{a_1}^2 - M_\pi^2 + \frac{t}{2}\right) D_{a_1}^{-1}\left[(p_- + k)^2\right] \qquad (2.10)\\
v_2 &= \frac{F_V G_V t}{F_\pi^2 M_\rho^2}\left\{-D_\rho^{-1}(t) - M_\rho^2 D_\rho^{-1}(t) D_\rho^{-1}\left[(P-q)^2\right]\right\} + \\
&\quad + \frac{F_V^2}{2F_\pi^2 M_\rho^2}\left\{-1 - M_\rho^2 D_\rho^{-1}\left[(P-q)^2\right] - (P-q)^2 D_\rho^{-1}\left[(P-q)^2\right]\right\} + \\
&\quad + \frac{F_A^2}{F_\pi^2 M_{a_1}^2}(M_{a_1}^2 - M_\pi^2 - p_-\cdot k) D_{a_1}^{-1}\left[(p_- + k)^2\right] \qquad (2.11)\\
v_3 &= \frac{F_A^2}{F_\pi^2 M_{a_1}^2} D_{a_1}^{-1}\left[(p_- + k)^2\right] \qquad (2.12)\\
v_4 &= -\frac{2F_V G_V}{F_\pi^2} D_\rho^{-1}(t) D_\rho^{-1}\left[(P-q)^2\right] + \frac{F_V^2}{F_\pi^2 M_\rho^2} D_\rho^{-1}\left[(P-q)^2\right]. \qquad (2.13)
\end{aligned}
$$

The resonance propagators are given by

$$
\begin{aligned}
D_\rho(t) &= M_\rho^2 - t - iM_\rho \Gamma_\rho(t) \\
D_{a_1}(t) &= M_{a_1}^2 - t - iM_{a_1}\Gamma_{a_1}(t) \qquad (2.14)
\end{aligned}
$$

in terms of the momentum dependent width [3]

$$
\Gamma_\rho(t) = \frac{M_\rho t}{96\pi F_\pi^2}\left[\left(1 - \frac{4M_\pi^2}{t}\right)^{3/2}\theta(t - 4M_\pi^2) + \frac{1}{2}\left(1 - \frac{4M_K^2}{t}\right)^{3/2}\theta(t - 4M_K^2)\right]. \qquad (2.15)
$$

JHEP08(2002)002

For $\Gamma_{a_1}(t)$ we use the parametrization of ref. [15]. Because of the already mentioned suppression of a_1 exchange neither the form of $\Gamma_{a_1}(t)$ nor its on-shell value (we take $\Gamma_{a_1}(M_{a_1}^2) = 0.5\,\mathrm{GeV}$) are of much importance in practice.

To define the decay amplitude (2.1) completely, we still have to specify the pion form factor $f_+(t)$. We use the results of ref. [3] where the chiral form factor of $O(p^4)$ was matched to the resonance region:

$$f_+(t) = M_\rho^2 D_\rho^{-1}(t) \exp\left[2\tilde{H}_{\pi\pi}(t) + \tilde{H}_{KK}(t)\right]. \tag{2.16}$$

The subtracted loop function $\tilde{H}_{PP}(t)$ is defined in appendix B.

The pion form factor (2.16) exhibits the correct low-energy behaviour to $O(p^4)$ by construction [3]. To check the low-energy limit of the vector amplitudes v_1, v_2 (v_3, v_4 arise only at $O(p^6)$), one has to insert the resonance dominance relations [2]

$$\begin{aligned} L_9 &= \frac{F_V G_V}{2M_\rho^2} \\ L_{10} &= \frac{F_A^2}{4M_{a_1}^2} - \frac{F_V^2}{4M_\rho^2}. \end{aligned} \tag{2.17}$$

3. Decay rate and spectrum

The differential rate for the decay $\tau^- \to \nu_\tau \pi^- \pi^0 \gamma$ is given by

$$\begin{aligned} d\Gamma &= \frac{1}{4m_\tau (2\pi)^8} \sum_{\text{spins}} |T|^2 d_{\text{LIPS}} \\ d_{\text{LIPS}} &= \frac{d^3q}{2E_\nu}\frac{d^3p_-}{2E_{\pi^-}}\frac{d^3p_0}{2E_{\pi^0}}\frac{d^3k}{2k^0}\delta^{(4)}(P - q - p_- - p_0 - k). \end{aligned} \tag{3.1}$$

The decay rate is dominated by bremsstrahlung of soft photons. To be sensitive to the dynamics of the proper radiative transition, a substantial cut on photon energies will be necessary.

We distinguish in the following between the full amplitude presented in the previous section and what we shall call "complete bremsstrahlung", i.e. the amplitude with

$$v_1 = v_2 = v_3 = v_4 = a_1 = a_2 = 0. \tag{3.2}$$

Since we use the expression (2.16) for the pion form factor in both cases, the correct Low limit (2.6) is guaranteed in both scenarios.

In table 1, we display the decay rate for three different lower cuts on the photon energy.

In figure 2 we compare the t-distribution for $E_\gamma \geq E_\gamma^{\min} = 300\,\mathrm{MeV}$ (in the τ rest frame) for the two options: the complete spectrum is shown as the full curve, the distribution corresponding to complete bremsstrahlung is given by the dashed curve. The interpretation of the spectrum is straightforward. The dominant peak is almost exclusively due to bremsstrahlung off the π^-. The secondary peak receives contributions from bremsstrahlung off the τ lepton but for a sufficiently high cut on the photon energy the spectrum is also sensitive to the additional resonance exchange contributions in $V_{\mu\nu}$ due to the diagrams in figure 6.

$E_\gamma^{\min}$ (MeV)	BR(full)	BR(brems)
100	$8.4 \cdot 10^{-4}$	$8.0 \cdot 10^{-4}$
300	$1.8 \cdot 10^{-4}$	$1.5 \cdot 10^{-4}$
500	$3.8 \cdot 10^{-5}$	$2.6 \cdot 10^{-5}$

Table 1: Branching ratios $BR(\tau^- \to \nu_\tau \pi^- \pi^0 \gamma)$ for different cuts $E_\gamma^{\min}$ on the photon energy. The second column corresponds to the full amplitude of section 2, the third one to the complete bremsstrahlung approximation defined in the text.

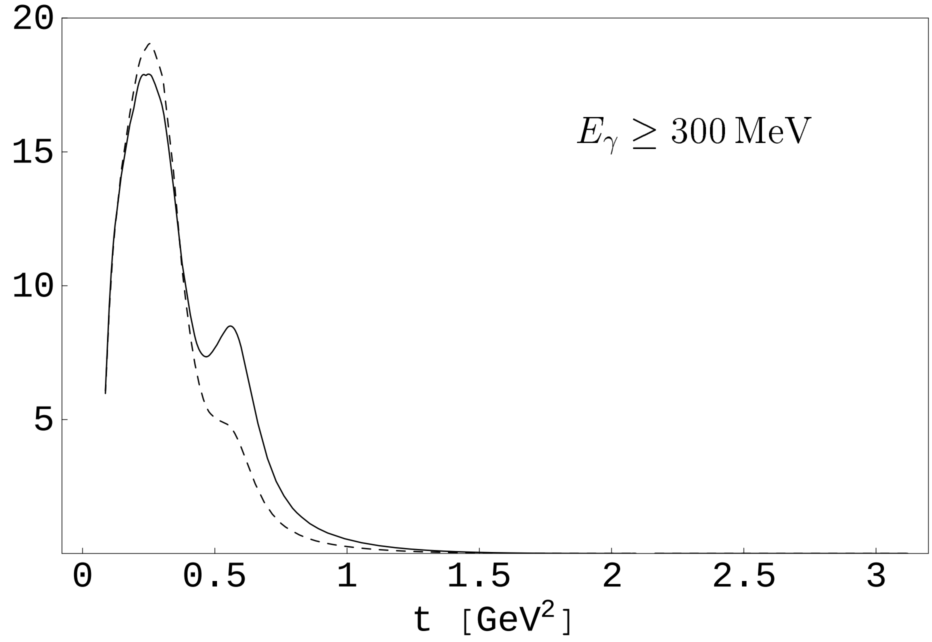

Figure 2: Decay spectrum (arbitrary units) as function of t, the invariant mass squared of the two pions, for photon energies bigger than $E_\gamma^{\min}$=300 MeV (in the τ rest frame): full amplitude (full curve) vs. complete bremsstrahlung (dashed curve).

There are at present no published results for the radiative decay under discussion. Table 1 and figure 2 suggest $E_\gamma^{\min} \sim 300$ MeV as a reasonable value for the cutoff in photon energy to test the nontrivial dynamics of the radiative decay. For smaller values, rate and spectrum become more and more dominated by (complete) bremsstrahlung. For larger cutoffs the branching ratios become too small.

We add a few comments on the theoretical status of the amplitude. Although our approach is well motivated from the low-energy structure predicted by QCD we cannot claim more than what it is worth: a realistic model for the intermediate-energy region that should be confronted with experiment. For instance, there is no guarantee that effects that only show up at $O(p^6)$ and higher in the low-energy expansion are fully accounted for. The situation is different for complete bremsstrahlung. In this case, the amplitude is completely determined by the pion form factor (2.16) which is known to describe the data very well in the region of interest [3]. Therefore, whenever complete bremsstrahlung dominates (for $E_\gamma^{\min} < 100$ MeV), rate and spectrum can be predicted in a model independent way.

4. Radiative corrections for hadronic vacuum polarization

The experimental precision in τ decays has made very accurate determinations of hadronic vacuum polarization possible. In particular, a precision of 1% has been achieved [16, 17] for the contribution of hadronic vacuum polarization to the anomalous magnetic moment of the muon. This accuracy makes a careful investigation of isospin violating and electromagnetic corrections mandatory.

In a recent letter [10], we have calculated the electromagnetic one-loop corrections for the two-pion decay of the τ lepton. Once the infrared divergences are removed by adding the decay rate due to soft photons, this loop correction is in principle well defined. However, a sizable uncertainty remains in general because the treatment of radiative events depends on the experimental setup. Without specifying those experimental conditions, we had to assign a rather big uncertainty to the radiative corrections. At best, the procedure of ref. [10] may be applied when only radiative events with photon energies below a sufficiently small energy cutoff are included. In this case, the leading Low approximation to the decay rate, as contained for instance in the widely used Monte Carlo program PHOTOS [18], may be expected to provide a first approximation. But even in this case, the specific value of the cutoff in photon energy would still have to be implemented in the analysis of ref. [10].

For the precision needed in the determination of hadronic vacuum polarization, a more careful analysis is mandatory. This is especially true for the case where all radiative events are included in the two-pion data sample as for instance in the ALEPH experiment [11]. When photons of all energies are considered the leading Low approximation for the radiative rate is of course no longer justified.

For this purpose, we will use the model of section 2 to calculate the radiative differential decay rate. To make the cancellation of infrared divergences transparent, we divide the calculation into two parts. The infrared divergent decay rate in leading Low approximation will be calculated analytically. When added to the equally infrared divergent electromagnetic one-loop correction [10] for the non-radiative decay, the infrared divergences cancel and the limit of vanishing photon mass can be taken. The second part of the radiative rate, containing in particular the subleading Low terms of $O(k^{-1})$, will be calculated numerically. This second part is infrared convergent and the photon mass can be set to zero from the start.

In the notation of our letter [10], we set out to calculate the electromagnetic correction function $G_{\rm EM}(t)$ defined by

$$\frac{d\Gamma_{\pi\pi[\gamma]}}{dt} = \frac{G_F^2 m_\tau^3 S_{\rm EW}|V_{ud}|^2}{384\pi^3}\left(1-\frac{4M_\pi^2}{t}\right)^{\frac{3}{2}}\left(1-\frac{t}{m_\tau^2}\right)^2\left(1+\frac{2t}{m_\tau^2}\right)|f_+(t)|^2\,G_{\rm EM}(t)\,. \quad (4.1)$$

The decay rate here is the fully inclusive one, i.e., with photons of all possible energies included. $S_{\rm EW}$ is a short-distance electroweak correction factor [19]. We also recall that we work in the isospin limit in this section.

In a first step, we consider only the leading Low approximation of $O(k^{-2})$ to the differential decay rate for the radiative process:

$$d\Gamma = \frac{\alpha G_F^2 |V_{ud}|^2}{32\pi^7 m_\tau} |f_+(t)|^2 D(t,u) \times \\ \times \left\{ \frac{2P\cdot p_-}{(P\cdot k - M_\gamma^2/2)(p_-\cdot k + M_\gamma^2/2)} - \frac{m_\tau^2}{(P\cdot k - M_\gamma^2/2)^2} - \frac{M_\pi^2}{(p_-\cdot k + M_\gamma^2/2)^2} \right\} d_{\rm LIPS}\,. \tag{4.2}$$

The kinematics of the radiative decay and the function $D(t,u)$ are given in appendix B. The Lorentz invariant phase space element $d_{\rm LIPS}$ is defined in eq. (3.1). Here and in the following, we neglect terms that will not contribute to the final result for $M_\gamma \to 0$.

Integration over neutrino and photon momenta leads to the three-fold differential rate

$$d\Gamma = \frac{\alpha G_F^2 |V_{ud}|^2}{64\pi^4 m_\tau^3} |f_+(t)|^2 D(t,u) \times \\ \times \left\{ 2P\cdot p_- I_{11}(t,u,x) - m_\tau^2 I_{20}(t,u,x) - M_\pi^2 I_{02}(t,u,x) \right\} dt\; du\; dx \tag{4.3}$$

with

$$I_{mn}(t,u,x) = \frac{1}{2\pi}\int \frac{d^3q}{2q^0}\frac{d^3k}{2k^0}\frac{\delta^{(4)}(P-q-p_- -p_0-k)}{(P\cdot k - M_\gamma^2/2)^m (p_-\cdot k + M_\gamma^2/2)^n}\,. \tag{4.4}$$

In the next step we perform the integration over x, the invariant mass squared of photon and neutrino. Here we must distinguish between two different regions in the $t-u$ plane. For (t,u) in the Dalitz plot of the non-radiative decay, the photon mass must be kept nonzero and the lower limit for the x-integration is in fact M_γ^2. For (t,u) that cannot be accessed in the non-radiative decay the lower limit is given by $x_-(t,u)$ in (B.5). The resulting contribution to the rate is infrared finite. The latter case can only occur for $t \le m_\tau^2 M_\pi/(m_\tau - M_\pi) = 0.27\,\mathrm{GeV}^2$. The corresponding contribution to the spectrum is very small. We will therefore not display the explicit formula for this part of the spectrum here but it will be included in the correction function $G_{\rm EM}(t)$. The upper limit of the x-integration is always given by $x_+(t,u)$ in (B.5).

The double differential decay rate in the leading Low approximation, for (t,u) in the non-radiative Dalitz plot and integrated over all photon momenta, takes the form

$$d\Gamma = \frac{\alpha G_F^2 |V_{ud}|^2}{64\pi^4 m_\tau^3} |f_+(t)|^2 D(t,u) \times \\ \times \left\{ J_{11}(t,u,M_\gamma) + J_{20}(t,u,M_\gamma) + J_{02}(t,u,M_\gamma) \right\} dt\; du\,. \tag{4.5}$$

Neglecting as always terms that vanish for $M_\gamma \to 0$, the functions J_{mn} are given by

$$\begin{aligned} J_{11}(t,u,M_\gamma) &= \log\left(\frac{2x_+(t,u)\bar\gamma}{M_\gamma}\right)\frac{1}{\bar\beta}\log\left(\frac{1+\bar\beta}{1-\bar\beta}\right) + \\ &\quad + \frac{1}{\bar\beta}\left\{ Li_2\left(\frac{1}{Y_2}\right) - Li_2(Y_1) + \log^2\frac{(-1/Y_2)}{4} - \log^2\frac{(-1/Y_1)}{4}\right\} \\ J_{20}(t,u,M_\gamma) &= \log\left(\frac{M_\gamma(m_\tau^2 - t)}{m_\tau x_+(t,u)}\right) \\ J_{02}(t,u,M_\gamma) &= \log\left(\frac{M_\gamma(m_\tau^2 + M_\pi^2 - t - u)}{M_\pi x_+(t,u)}\right). \end{aligned} \tag{4.6}$$

The various quantities in these functions are defined in appendix B.

The remaining part of the radiative decay rate, containing all terms except the leading Low terms, is calculated numerically. Putting everything together, the double differential rate for the photon-inclusive two-pion decay is given by

$$\frac{d\Gamma_{\pi\pi[\gamma]}}{dt\ du} = \frac{G_F^2 S_{\rm EW}|V_{ud}|^2}{64\pi^3 m_\tau^3}|f_+(t)|^2 D(t,u)\left\{1+2f_{\rm loop}^{\rm elm}(u,M_\gamma)+g_{\rm rad}(t,u,M_\gamma)\right\}. \qquad (4.7)$$

The electromagnetic loop amplitude $f_{\rm loop}^{\rm elm}(u,M_\gamma)$ was calculated in ref. [10] and is reproduced in appendix B. The radiative part of the rate is determined by the function $g_{\rm rad}(t,u,M_\gamma)$ with

$$g_{\rm rad}(t,u,M_\gamma) = g_{\rm brems}(t,u,M_\gamma)+g_{\rm rest}(t,u) \qquad (4.8)$$

$$g_{\rm brems}(t,u,M_\gamma) = \frac{\alpha}{\pi}[J_{11}(t,u,M_\gamma)+J_{20}(t,u,M_\gamma)+J_{02}(t,u,M_\gamma)]\,. \qquad (4.9)$$

The (numerically calculated) function $g_{\rm rest}(t,u)$ accounts for the infrared finite remainder of the rate, i.e., all terms except the ones contained in $g_{\rm brems}(t,u,M_\gamma)$. As it must be, the sum $2f_{\rm loop}^{\rm elm}+g_{\rm brems}$ is independent of the photon mass and therefore infrared finite as well.

To obtain the correction function $G_{\rm EM}(t)$, we still have to integrate over u [10]:

$$G_{\rm EM}(t) = \frac{\int_{u_{\rm min}(t)}^{u_{\rm max}(t)} du\, D(t,u)\,\Delta(t,u)}{\int_{u_{\rm min}(t)}^{u_{\rm max}(t)} du\, D(t,u)}\,, \qquad (4.10)$$

with

$$\Delta(t,u) = 1+2f_{\rm loop}^{\rm elm}(u,M_\gamma)+g_{\rm brems}(t,u,M_\gamma)+g_{\rm rest}(t,u)\,. \qquad (4.11)$$

The limits of integration $u_{\rm min,max}(t)$ can also be found in appendix B.

Since only the sum $2f_{\rm loop}^{\rm elm}+g_{\rm brems}$ is physically meaningful two distinct pieces can be distinguished in $G_{\rm EM}(t)$. Setting $g_{\rm rest}$ to zero, we obtain a function $G_{\rm EM}^{(0)}(t)$ that describes radiative corrections in the leading Low approximation. In figure 3 we plot both the complete result $G_{\rm EM}(t)$ and the (leading) bremsstrahlung approximation $G_{\rm EM}^{(0)}(t)$.

The obvious conclusion is that the non-leading terms in the Low expansion cannot be neglected when considering the photon-inclusive spectrum and rate. One should keep in mind that the function $G_{\rm EM}(t)$ multiplies the non-radiative spectrum in (4.1) that is strongly peaked around $t=M_\rho^2\simeq 0.6\,{\rm GeV}^2$.

Where does the difference between the two curves in figure 3 mainly come from? The answer is that it comes almost exclusively from the subleading Low terms in (2.6). In other words, the amplitudes $v_1,\ldots,v_4,a_1,a_2$ have practically no impact on $G_{\rm EM}(t)$. In fact, $G_{\rm EM}(t)$ for

$$v_1=v_2=v_3=v_4=a_1=a_2=0$$

could not be distinguished from the full result in figure 3. This conclusion corresponds to the findings in section 3 that the specific features of the model for the radiative transition only show up for a sufficiently large lower cut on photon energies.

In the present case where photons of all energies are included, complete bremsstrahlung is an excellent approximation. However, as figure 3 documents very clearly, the leading

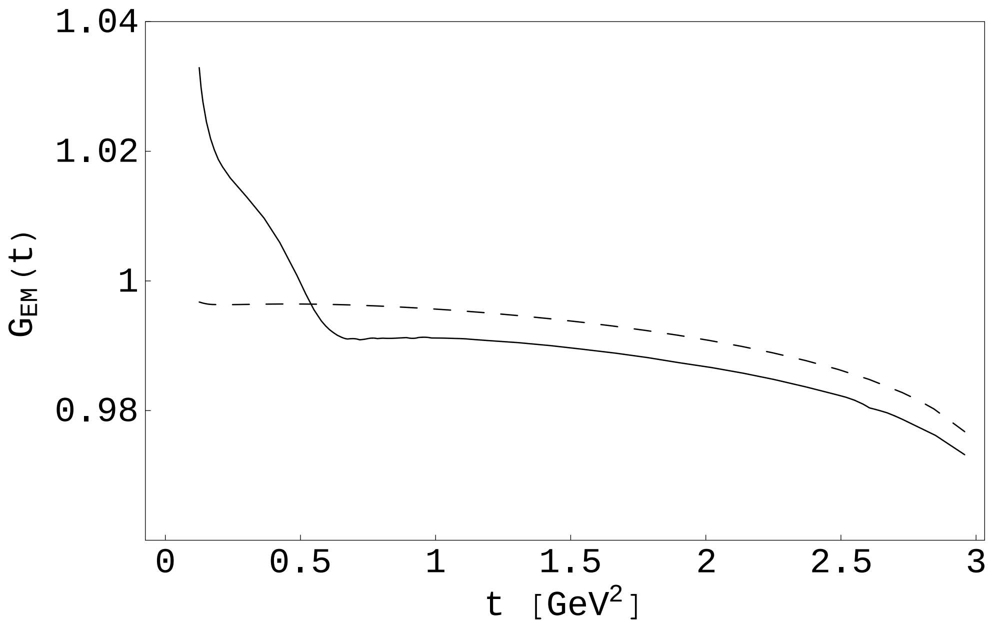

Figure 3: Correction function $G_{\rm EM}(t)$ defined in (4.1) and (4.10). The full curve corresponds to the complete radiative amplitude, the dashed curve describes the leading Low approximation.

Low approximation ($O(k^{-2})$ in rate) corresponding to the function $G_{\rm EM}^{(0)}(t)$ is not a valid approximation. The complete bremsstrahlung approximation ($v_1 = v_2 = v_3 = v_4 = a_1 = a_2 = 0$ in (2.4), (2.5)) is uniquely determined by the pion form factor $f_+(t)$. The correction function $G_{\rm EM}(t)$ is therefore effectively independent of the details of the model of section 2 for the radiative transition.

Finally, we emphasize once again that the analysis in this section applies to the photon-inclusive case only. Moreover, even the leading Low approximation $G_{\rm EM}^{(0)}(t)$ (dashed curve in figure 3) cannot be compared directly with the corresponding function in ref. [10] that contained only the loop contribution (with an ad hoc prescription for the infrared divergent part). In contrast, the curves in figure 3 refer to the complete electromagnetic corrections, i.e., to the (infrared finite) sum of loop and radiative contributions with photons of all energies included.

5. Isospin violating corrections for a_μ

The leading hadronic contribution to the anomalous magnetic moment of the muon $a_\mu = (g_\mu - 2)/2$ is due to hadronic vacuum polarization [20],

$$a_\mu^{\rm vacpol} = \frac{1}{4\pi^3} \int_{4M_\pi^2}^\infty dt K(t) \sigma^0_{e^+e^- \to {\rm hadrons}}(t) \,, \tag{5.1}$$

where $K(t)$ is a smooth kernel concentrated at low energies and $\sigma^0_{e^+e^- \to {\rm hadrons}}$ denotes the bare hadronic cross section with QED corrections removed. The low-energy structure of hadronic vacuum polarization is especially important. In fact, about 70 % of $a_\mu^{\rm vacpol}$ is due to the two-pion intermediate state for $4M_\pi^2 \le t \le 0.8\,\mathrm{GeV}^2$ (see, e.g., ref. [21]). A substantial improvement in the accuracy is possible if one includes data from hadronic τ decays. A precise link between hadronic spectral functions from τ decays and from the e^+e^- hadronic cross section requires the calculation of radiative corrections as well as the inclusion of other isospin breaking effects (both kinematical and dynamical in origin). For the two-pion final state, we have parameterized [10] the relation between the *bare* e^+e^- cross section and the *observed* differential τ decay rate as follows:[2]

$$\sigma^0_{\pi\pi} = \left[\frac{K_\sigma(t)}{K_\Gamma(t)}\,\frac{d\Gamma_{\pi\pi[\gamma]}}{dt}\right] \times \frac{R_{\rm IB}(t)}{S_{\rm EW}}\,, \tag{5.2}$$

where

$$\begin{aligned} K_\Gamma(t) &= \frac{G_F^2\,|V_{ud}|^2\,m_\tau^3}{384\pi^3}\left(1-\frac{t}{m_\tau^2}\right)^2\left(1+2\frac{t}{m_\tau^2}\right) \\ K_\sigma(t) &= \frac{\pi\,\alpha^2}{3\,t} \end{aligned} \tag{5.3}$$

and the isospin breaking correction is in

$$R_{\rm IB}(t) = \frac{1}{G_{\rm EM}(t)}\,\frac{\beta^3_{\pi^+\pi^-}}{\beta^3_{\pi^+\pi^0}}\,\left|\frac{F_V(t)}{f_+(t)}\right|^2 . \tag{5.4}$$

The factor $S_{\rm EW} = 1.0194$ (taken at the scale m_τ) takes into account the dominant short-distance electroweak corrections [19]. $R_{\rm IB}(t)$ involves the long-distance QED correction $G_{\rm EM}(t)$ (discussed in detail in the previous section), the phase space correction factor $\beta^3_{\pi^+\pi^-}(t)/\beta^3_{\pi^0\pi^-}(t)$ (important in the low-t region), and the ratio of electromagnetic (F_V) over weak (f_+) pion form factors.

In this section we discuss the isospin breaking affecting the ratio of form factors. Since our purpose is to relate the observed weak decay to the bare two-pion cross section, we need to include effects of order $(m_u - m_d)$ in both F_V and f_+, while we need explicit photonic corrections of order α only in f_+. Keeping track of all relevant sources of isospin breaking at first order, eq. (2.16) generalizes to

$$F_V(t) = M^2_{\rho^0} D^{-1}_{\rho^0}(t)\left[\exp\left(2\tilde H_{\pi^+\pi^-}(t) + \tilde H_{K^+K^-}(t)\right) - \frac{\theta_{\rho\omega}}{3M_\rho^2}\,\frac{t}{M_\omega^2 - t - iM_\omega\Gamma_\omega}\right] \tag{5.5}$$

$$f_+(t) = M^2_{\rho^+} D^{-1}_{\rho^+}(t)\,\exp\left(2\tilde H_{\pi^+\pi^0}(t) + \tilde H_{K^+K^0}(t)\right) + f^{\rm elm}_{\rm local} + \ldots \tag{5.6}$$

In eq. (5.5) the main new ingredient compared to ref. [10] is the inclusion of the ω contribution to the electromagnetic form factor, following the notation of ref. [22]. This contribution was not included in our previous work [10] because it is formally of higher order in the

[2] The bare e^+e^- cross section directly provides the two-pion contribution to the muon $g-2$ at $O(\alpha^2)$. We follow here the tacit convention that only explicit photonic corrections are considered in the counting of powers of α. In other words, electromagnetic contributions to the charged pion mass or to ρ-ω mixing are included in the lowest-order contribution of $O(\alpha^2)$.

low-energy expansion. Here we include ρ-ω mixing together with all other numerically relevant isospin violating contributions. The mixing parameter can be extracted from the decay width for $\omega \to \pi^+\pi^-$ leading to $\theta_{\rho\omega} = (-3.9 \pm 0.3) \cdot 10^{-3}\,\mathrm{GeV}^2$ in the framework of ref. [22]. A more direct determination comes from the recent Novosibirsk data for $e^+e^- \to \pi^+\pi^-$ [23]. Translating their fit for the mixing parameter into our notation gives $\theta_{\rho\omega} = (-3.3 \pm 0.5) \cdot 10^{-3}\ \mathrm{GeV}^2$ (the same value has been obtained in an independent fit of the CMD-2 data [24]). For the numerical discussion we take $\theta_{\rho\omega} = (-3.5 \pm 0.7) \cdot 10^{-3}\ \mathrm{GeV}^2$. For the remaining parameters we use $M_\omega = 0.783\,\mathrm{GeV}$ and $\Gamma_\omega = 0.00844\,\mathrm{GeV}$.

Equation (5.6) reproduces our previous result [10] where $f^{\rm elm}_{\rm local}$ represents the structure dependent electromagnetic corrections to the low-t part of the spectrum:

$$f^{\rm elm}_{\rm local} = \frac{\alpha}{4\pi}\bigg[-\frac{3}{2} - \frac{1}{2}\log\frac{m_\tau^2}{\mu^2} - \log\frac{M_\pi^2}{\mu^2} + 2\log\frac{m_\tau^2}{M_\rho^2} - \\ - (4\pi)^2\left(-2K_{12}^r(\mu) + \frac{2}{3}X_1 + \frac{1}{2}\tilde{X}_6^r(\mu)\right)\bigg]. \tag{5.7}$$

K_{12}, X_1 and X_6 are LECs appearing in the effective lagrangian of CHPT. Numerical estimates for the chiral couplings are reported in ref. [10]. The dots in eq. (5.6) represent unknown structure dependent corrections to the form factor, away from the threshold region. At the moment there is no model independent method for including such terms. However, our calculation correctly identifies the large UV logs (in $S_{\rm EW}$) and the IR logs (chiral logs in $f^{\rm elm}_{\rm local}$ and $f^{\rm elm}_{\rm loop}$), and therefore the neglected terms are expected to be numerically smaller.

In the numerical analysis we also account for isospin violating effects due to mass and width differences between the charged and the neutral ρ mesons. The ρ^+-ρ^0 mass difference is unknown but expected to be small [25, 11]. We follow ref. [16] and assume $M_{\rho^+} - M_{\rho^0} = (0 \pm 1)$ MeV. In addition to the two-pion contributions, there is also a possible width difference due to radiative decays, dominated by the $\pi\pi\gamma$ modes. We include the measured $\pi\pi\gamma$ decay width of the ρ^0 of approximately 1.5 MeV [26] and assume a radiative decay width difference $\Gamma(\rho^0 \to \pi^+\pi^-\gamma) - \Gamma(\rho^+ \to \pi^+\pi^0\gamma) = (0.45 \pm 0.45)$ MeV [27, 5, 16].

We can summarize our results graphically. In figure 4 we plot the ratio $|F_V/f_+|^2$ showing the sensitivity to $\theta_{\rho\omega}$. In figure 5 we plot the full isospin violating correction function $R_{\rm IB}(t)$ containing the complete radiative correction $G_{\rm EM}(t)$, displaying also the small uncertainty due to the electromagnetic LECs.

In order to investigate the impact of $R_{\rm IB}(t)$ on $a_\mu^{\rm vacpol}$, we have evaluated for the two-pion contribution to (5.1) the difference between the correct expression for $\sigma^0_{\pi\pi}$ (full r.h.s. of eq. (5.2)) and the naive CVC expression (the term in square brackets on the r.h.s. of (5.2)), up to a scale $t_{\rm max}$:

$$\Delta a_\mu^{\rm vacpol} = \frac{1}{4\pi^3}\int_{4M_\pi^2}^{t_{\rm max}} dt K(t)\,\left[\frac{K_\sigma(t)}{K_\Gamma(t)}\,\frac{d\Gamma_{\pi\pi[\gamma]}}{dt}\right] \times \left(\frac{R_{\rm IB}(t)}{S_{\rm EW}} - 1\right). \tag{5.8}$$

In table 2, we have analysed separately the effects of $S_{\rm EW}$ and of the three ingredients of R_{IB}: kinematics (KIN), radiative correction (EM) and form factor ratio (FF). We find that the difference $\Delta a_\mu^{\rm vacpol}$ is quite insensitive to $t_{\rm max}$ as long as $t_{\rm max} \geq 1\,\mathrm{GeV}^2$ (cf. table 2). We can summarize our results as follows:

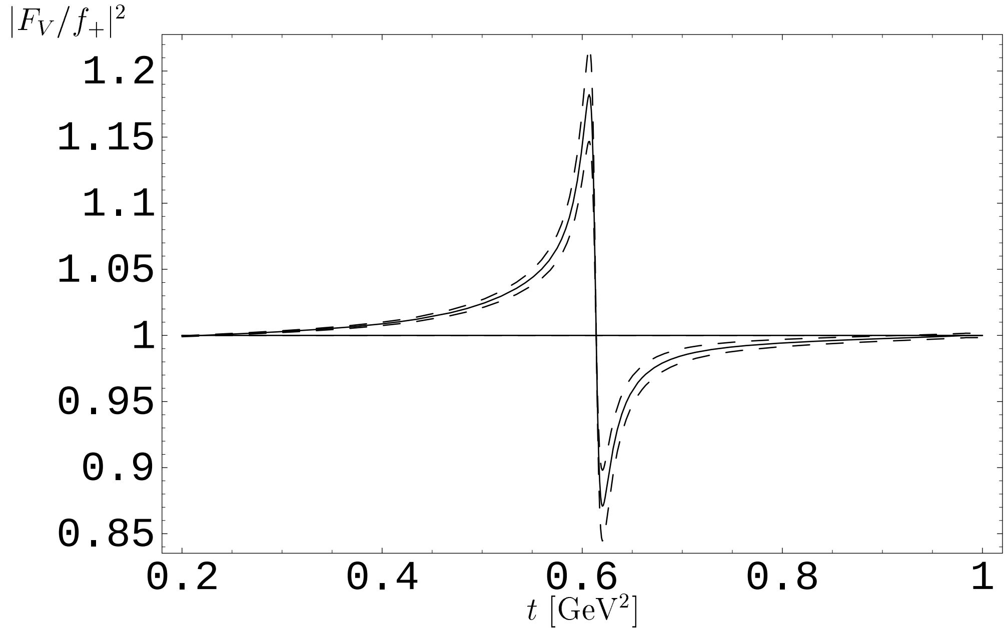

Figure 4: The ratio $|F_V/f_+|^2$ for $\theta_{\rho\omega} = (-3.5 \pm 0.7) \cdot 10^{-3}\,\mathrm{GeV}^2$. The full curve corresponds to the mean value. For this plot we have assumed $M_{\rho^+} = M_{\rho^0} = 775\,\mathrm{MeV}$ and we have neglected the radiative decay widths.

$t_{\max}$	S_{EW}	KIN	EM	FF	$\Delta a_\mu^{\mathrm{vacpol}}$ (total)
1	-95	-75	-11	$61 \pm 26 \pm 3$	-119
2	-97	-75	-10	$61 \pm 26 \pm 3$	-120
3	-97	-75	-10	$61 \pm 26 \pm 3$	-120

Table 2: Contributions to $\Delta a_\mu^{\mathrm{vacpol}}$ from various sources of isospin violation (in units of 10^{-11}) for different values of $t_{\max}$ (in units of GeV^2) as defined in eq. (5.8).

- The short-distance correction $S_{\mathrm{EW}} = 1.0194$ induces $\Delta a_\mu^{\mathrm{vacpol}} = -97 \cdot 10^{-11}$.
- The kinematical effect induces a shift $\Delta a_\mu^{\mathrm{vacpol}} = -75 \cdot 10^{-11}$.
- The complete radiative corrections produce a shift $\Delta a_\mu^{\mathrm{vacpol}} = -10 \cdot 10^{-11}$. We emphasize once more that this correction applies only for the case of a photon-inclusive two-pion data set as provided for instance by the ALEPH experiment [11]. If we had used the leading Low correction factor $G_{\mathrm{EM}}^{(0)}(t)$, the shift would be $\Delta a_\mu^{\mathrm{vacpol}} = +16 \cdot 10^{-11}$ instead.
- The ratio of form factors produces a positive shift of approximately $61{\cdot}10^{-11}$. Roughly 60 % of this effect is due to ρ-ω mixing, the remainder comes from the ρ^+-ρ^0 width difference (pion mass difference and radiative decay modes). We add the errors due to the previously discussed uncertainties of ρ-ω mixing (8), ρ^+-ρ^- mass difference (20) and radiative decay widths (14) in quadrature (the numbers in brackets denote

JHEP08(2002)002

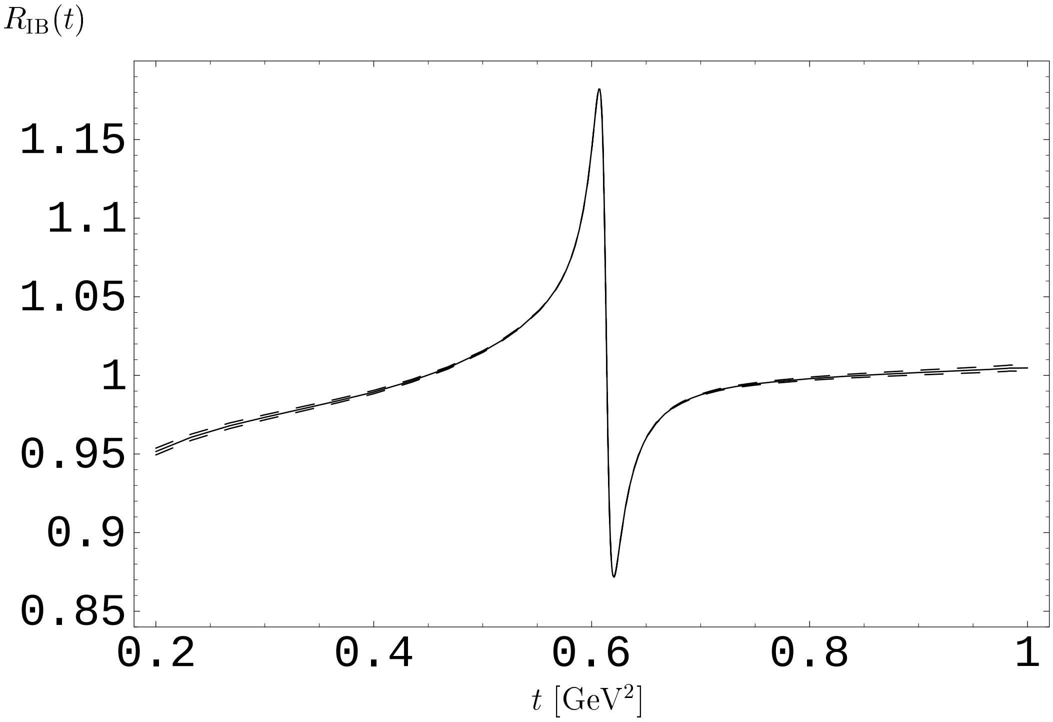

Figure 5: Full correction factor $R_{\rm IB}(t)$ with the complete radiative correction $G_{\rm EM}(t)$ (solid curve). The (almost indistinguishable) dashed curves correspond to variation of the chiral couplings within their error bars [10]. In this plot we use $\theta_{\rho\omega} = -3.5 \cdot 10^{-3}\,{\rm GeV}^2$, ρ masses and widths as in figure 4.

the corresponding shifts in units of 10^{-11}), but keep the small additional uncertainty in the electromagnetic LECs [10] (3) separate. The final shift due to the form factor ratio is therefore $\Delta a_\mu^{\rm vacpol} = +(61 \pm 26 \pm 3) \cdot 10^{-11}$.

Our results are based on the form factor representations of eqs. (5.5) and (5.6). Use of the experimentally measured f_+, as well as a different treatment of the form factor ratio [16], produce slightly different values for the individual contributions to $\Delta a_\mu^{\rm vacpol}$. The overall picture emerging from the two treatments is however quite consistent: there is a strong cancellation of all effects included in $R_{\rm IB}(t)$. The results in table 2 put this statement on a quantitative basis.

Collecting all isospin violating contributions, we obtain finally

$$\Delta a_\mu^{\rm vacpol} = (-120 \pm 26 \pm 3) \cdot 10^{-11}\,. \tag{5.9}$$

We have not assigned an error for the short-distance correction factor S_{EW} because this is already included in the error for the electromagnetic LECs. S_{EW} is in fact closely related to the LEC $X_6^r(M_\rho)$ after scaling it down from m_τ to M_ρ [10, 28]. Altogether, we are confident that with the photon-inclusive two-pion decay of the τ as input the isospin breaking shift (5.9) can be given to an accuracy of about 20%. The accuracy could be improved considerably by better determinations of the ρ mass and radiative decay width differences.

6. Conclusions

Guided by the low-energy limit dictated by CHPT, we have constructed a meson resonance model which allows the investigation of the radiative τ decay $\tau^- \to \nu_\tau \pi^- \pi^0 \gamma$ for the whole range of momentum transfer to the hadronic system. We have shown that for a photon energy cut of approximately 300 MeV in the τ rest frame, the nontrivial part of the amplitude can be discriminated from the pure bremsstrahlung contribution in the decay spectrum.

As a second application of our model, we have considered the radiative corrections for the process $\tau^- \to \nu_\tau \pi^- \pi^0$. This includes also real photon emission via the associated radiative decay. Such an investigation is relevant once experimental data from hadronic τ decays are used for the determination of the hadronic vacuum polarization, which requires a reliable estimate of isospin violating effects.

The contribution from real photon emission to the decay rate depends on the experimental setup. If photons of all energies are included (as in the ALEPH data [11]), the leading Low approximation is definitely not sufficient any more. On the other hand, complete bremsstrahlung turns out to be an excellent approximation in this case. Compared to the naive CVC relation, we find a total isospin violating shift of the anomalous magnetic moment of the muon a_μ of $\Delta a_\mu^{\rm vacpol} = (-120 \pm 26 \pm 3) \cdot 10^{-11}$. The first error is due to the combined uncertainties of ρ-ω mixing, ρ^+-ρ^0 mass and (radiative decay) width differences. The comparatively small second error is based on available estimates of the low-energy constants.

Acknowledgments

We thank Michel Davier and Andreas Höcker for helpful discussions and for information on the data analysis of the ALEPH experiment. We are grateful to Jorge Portolés for pointing out to us the new determination of the ρ-ω mixing angle by the CMD-2 collaboration. The work of V.C. has been supported in part by MCYT, Spain (Grant No. FPA-2001-3031) and by ERDF funds from the European Commission.

A. Resonance contributions

The resonance exchange contributions considered in section 2 are derived from the standard chiral resonance lagrangian [2] for vector and axial-vector mesons (scalar exchange does not contribute to our decay):

$$\mathcal{L}[V(1^{--}), A(1^{++})] = \mathcal{L}_{\rm kin}[V, A] + \frac{F_V}{2\sqrt{2}} \langle V_{\mu\nu} f_+^{\mu\nu} \rangle + \frac{iG_V}{\sqrt{2}} \langle V_{\mu\nu} u^\mu u^\nu \rangle + \frac{F_A}{2\sqrt{2}} \langle A_{\mu\nu} f_-^{\mu\nu} \rangle \, . \quad \text{(A.1)}$$

The lagrangian is formulated in terms of SU(3) tensor fields $V_{\mu\nu}, A_{\mu\nu}$ (not to be confused with the tensor amplitudes of section 2). We refer to ref. [2] for definitions and further details, in particular for the explicit form of the gauge and chiral invariant kinetic terms that contain the couplings bilinear in the resonance fields.

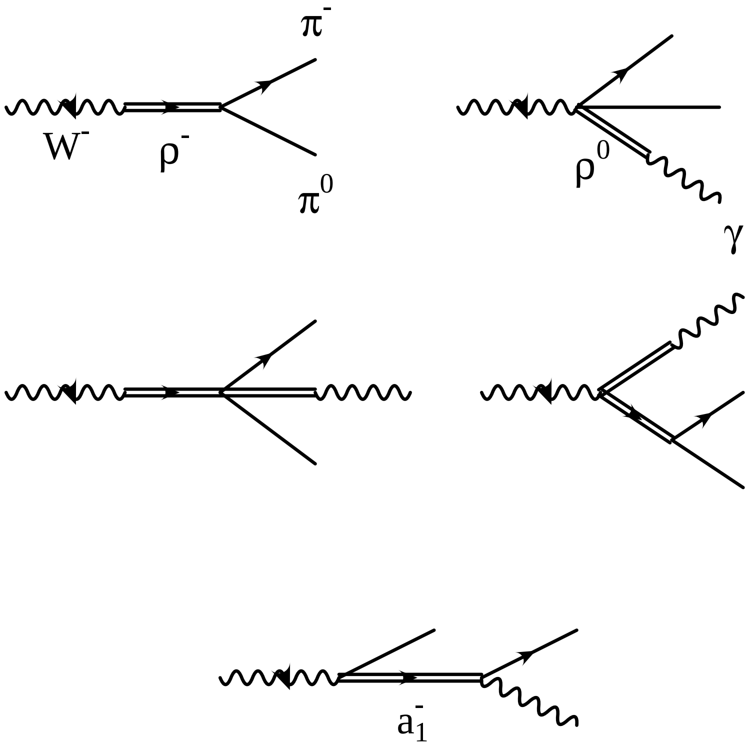

Figure 6: ρ and a_1 exchange diagrams for the model of section 2. In the first diagram, a photon is to be appended wherever possible.

In addition to $M_\rho = 0.775\,\mathrm{GeV}$, $M_{a_1} = 1.23\,\mathrm{GeV}$ and $\Gamma_{a_1} = 0.5\,\mathrm{GeV}$ we use for the resonance couplings the theoretically favoured values [29]

$$F_V = \sqrt{2}F_\pi = 0.13\,\mathrm{GeV}\,, \qquad G_V = F_\pi/\sqrt{2} = 0.065\,\mathrm{GeV}\,, \qquad F_A = F_\pi = 0.0924\,\mathrm{GeV}\,.$$

These values for F_V, G_V are used in the energy dependent width (2.14) leading to $\Gamma_\rho = \Gamma_\rho(M_\rho^2) = 0.147$ GeV.

The vector amplitudes $v_1, \ldots, v_4$ are derived from the diagrams in figure 6.

B. Kinematics and loop corrections

B.1 Kinematics

After integration over neutrino and photon 4-momenta, the spin-averaged decay distribution for

$$\tau^-(P) \to \nu_\tau(q)\pi^-(p_1)\pi^0(p_2)\gamma(k)$$

depends on three invariants.[3] We use

$$t = (p_1 + p_2)^2\,, \qquad u = (P - p_1)^2\,, \qquad x = (q + k)^2 \tag{B.1}$$

[3] In the body of the text we use the more suggestive notation $p_1 = p_-$, $p_2 = p_0$.

JHEP08(2002)002

with $P^2 = m_\tau^2$, $p_i^2 = M_i^2$ $(i = 1, 2)$. In order to calculate differential rates and spectra, we need the physical region $\mathcal{D}$ in the form of a normal domain:

$$\mathcal{D} = \{t_{\min} \leq t \leq t_{\max}\,,\ u_{\min}(t) \leq u \leq u_{\max}(t)\,,\ x_{\min}(t,u) \leq x \leq x_{\max}(t,u)\}\,, \tag{B.2}$$

where

$$t_{\min} = (M_1 + M_2)^2\,, \qquad t_{\max} = m_\tau^2\,. \tag{B.3}$$

In order to give the explicit form of $u_{\min/\max}(t)$ and $x_{\min/\max}(t,u)$ we introduce the auxiliary functions

$$\begin{aligned} u_\pm(t,x) \;=\; & \frac{1}{2\,t}\Bigg[2\,t\,(m_\tau^2 + M_1^2) - (t + M_1^2 - M_2^2)\,(m_\tau^2 + t - x) \pm \\ & \qquad \pm \sqrt{\lambda(t, M_1^2, M_2^2)\,\lambda(m_\tau^2, t, x)}\Bigg] \end{aligned} \tag{B.4}$$

$$\begin{aligned} x_\pm(t,u) \;=\; & \frac{1}{2\,M_1^2}\Bigg[2\,M_1^2\,(m_\tau^2 + t) - (t + M_1^2 - M_2^2)\,(m_\tau^2 + M_1^2 - u) \pm \\ & \qquad \pm \sqrt{\lambda(t, M_1^2, M_2^2)\,\lambda(u, M_1^2, m_\tau^2)}\Bigg] \end{aligned} \tag{B.5}$$

with $\lambda(x,y,z) \;=\; x^2 + y^2 + z^2 - 2\,(xy + xz + yz)$. In the following, let us call $\mathcal{R}^{III}$ the region in the t-u plane accessible in the non-radiative three-body decay, and $\mathcal{R}^{IV}$ the region accessible in the radiative decay. $\mathcal{R}^{III}$ is given by

$$\bar{u}_{\min}(t) \;=\; u_-(t,0) \qquad \text{for} \quad t_{\min} \leq t \leq t_{\max} \tag{B.6}$$

$$\bar{u}_{\max}(t) \;=\; u_+(t,0) \qquad \text{for} \quad t_{\min} \leq t \leq t_{\max} \tag{B.7}$$

while $\mathcal{R}^{IV}$ corresponds to

$$u_{\min}(t) \;=\; u_-(t,0) \qquad \text{for} \quad t_{\min} \leq t \leq t_{\max} \tag{B.8}$$

$$u_{\max}(t) \;=\; \begin{cases} u_+(t,0) & \text{for} \quad t_* \leq t \leq t_{\max} \\ (m_\tau - M_1)^2 & \text{for} \quad t_{\min} \leq t \leq t_* \end{cases} \tag{B.9}$$

with

$$t_* = \frac{m_\tau(m_\tau M_1 + M_2^2 - M_1^2)}{m_\tau - M_1}\,. \tag{B.10}$$

Finally, for given (t,u) the limits for x are

$$x_{\max}(t,u) \;=\; x_+(t,u) \tag{B.11}$$

$$x_{\min}(t,u) \;=\; \begin{cases} M_\gamma^2 & \text{for} \quad (t,u) \in \mathcal{R}^{III} \\ x_-(t,u) & \text{for} \quad (t,u) \in \mathcal{R}^{IV} \setminus \mathcal{R}^{III}\,. \end{cases} \tag{B.12}$$

The differential decay rate in eq. (4.5) involves the function

$$D(t,u) = \frac{m_\tau^2}{2}(m_\tau^2 - t) + 2M_1^2 M_2^2 - 2\,u\,(m_\tau^2 - t + M_1^2 + M_2^2) + 2\,u^2\,. \tag{B.13}$$

Moreover, the following combinations of invariants appear in eq. (4.6):

$$Y_{1,2} = \frac{1 - 2\bar{\alpha} \pm \sqrt{(1-2\bar{\alpha})^2 - (1-\bar{\beta}^2)}}{1+\bar{\beta}}\,, \tag{B.14}$$

with

$$\begin{aligned}
\bar{\alpha} &= \frac{(m_\tau^2 - t)(m_\tau^2 + M_2^2 - t - u)}{(M_1^2 + m_\tau^2 - u)} \cdot \frac{\lambda(u, M_1^2, m_\tau^2)}{2\,\bar{\delta}} \\
\bar{\beta} &= -\frac{\sqrt{\lambda(u, M_1^2, m_\tau^2)}}{M_1^2 + m_\tau^2 - u} \\
\bar{\gamma} &= \frac{\sqrt{\lambda(u, M_1^2, m_\tau^2)}}{2\sqrt{\bar{\delta}}} \\
\bar{\delta} &= -M_2^4 m_\tau^2 + M_1^2 (m_\tau^2 - t)(M_2^2 - u) - tu(-m_\tau^2 + t + u) + \\
&\quad + M_2^2(-m_\tau^4 + tu + m_\tau^2 t + m_\tau^2 u)
\end{aligned}$$

B.2 Loop functions

The loop function $\tilde{H}_{PQ}(t, \mu)$ is given by

$$\begin{aligned}
\tilde{H}_{PQ}(t,\mu) &= \frac{1}{F^2}\mathcal{R}e\Bigg[\frac{1}{12t}\lambda(t, M_P^2, M_Q^2)\,\bar{J}^{PQ}(t) + \frac{1}{18(4\pi)^2}(t - 3\Sigma_{PQ}) - \\
&\quad - \frac{1}{12}\left(\frac{2\Sigma_{PQ} - t}{\Delta_{PQ}}(A_P(\mu) - A_Q(\mu)) - 2(A_P(\mu) + A_Q(\mu))\right)\Bigg]\,,
\end{aligned} \tag{B.15}$$

where

$$\begin{aligned}
\Sigma_{PQ} &= M_P^2 + M_Q^2\,, \qquad \Delta_{PQ} = M_P^2 - M_Q^2 \\
A_P(\mu) &= -\frac{M_P^2}{(4\pi)^2}\log\frac{M_P^2}{\mu^2} \\
\bar{J}^{PQ}(t) &= \frac{1}{32\pi^2}\Bigg[2 + \frac{\Delta_{PQ}}{t}\log\frac{M_Q^2}{M_P^2} - \frac{\Sigma_{PQ}}{\Delta_{PQ}}\log\frac{M_Q^2}{M_P^2} - \\
&\quad - \frac{\lambda^{1/2}(t, M_P^2, M_Q^2)}{t}\log\left(\frac{(t + \lambda^{1/2}(t, M_P^2, M_Q^2))^2 - \Delta_{PQ}^2}{(t - \lambda^{1/2}(t, M_P^2, M_Q^2))^2 - \Delta_{PQ}^2}\right)\Bigg]\,.
\end{aligned} \tag{B.16}$$

The one-loop virtual photon correction, contributing to the differential spectrum (4.7), is given by[4]

$$\begin{aligned}
f_{\rm loop}^{\rm elm}(u, M_\gamma) &= \frac{\alpha}{4\pi}\Bigg[(u - M_\pi^2)\,\mathcal{A}(u) + (u - M_\pi^2 - m_\tau^2)\,\mathcal{B}(u) + \\
&\quad + 2\,(M_\pi^2 + m_\tau^2 - u)\,\mathcal{C}(u, M_\gamma) + 2\,\log\frac{M_\pi m_\tau}{M_\gamma^2}\Bigg]\,.
\end{aligned} \tag{B.17}$$

[4]The last term in $f_{\rm loop}^{\rm elm}(u, M_\gamma)$ was missing from eq. (16) of ref. [10]. This typo did not affect the numerical analysis of ref. [10].

In terms of the variables

$$r_\tau = \frac{m_\tau^2}{M_\pi^2}, \qquad y_\tau = 1 + r_\tau - \frac{u}{M_\pi^2}, \qquad x_\tau = \frac{1}{2\sqrt{r_\tau}}(y_\tau - \sqrt{y_\tau^2 - 4r_\tau}), \tag{B.18}$$

and of the dilogarithm

$$Li_2(z) = -\int_0^1 \frac{dt}{t}\log(1 - zt), \tag{B.19}$$

the functions contributing to $f_{\rm loop}^{\rm elm}(u, M_\gamma)$ are given by

$$\mathcal{A}(u) = \frac{1}{u}\left[-\frac{1}{2}\log r_\tau + \frac{2 - y_\tau}{\sqrt{r_\tau}}\frac{x_\tau}{1 - x_\tau^2}\log x_\tau\right] \tag{B.20}$$

$$\mathcal{B}(u) = \frac{1}{u}\left[\frac{1}{2}\log r_\tau + \frac{2r_\tau - y_\tau}{\sqrt{r_\tau}}\frac{x_\tau}{1 - x_\tau^2}\log x_\tau\right] \tag{B.21}$$

$$\begin{aligned}\mathcal{C}(u, M_\gamma) = \frac{1}{m_\tau M_\pi}\frac{x_\tau}{1 - x_\tau^2}\Bigg[&-\frac{1}{2}\log^2 x_\tau + 2\log x_\tau \log(1 - x_\tau^2) - \frac{\pi^2}{6} + \frac{1}{8}\log^2 r_\tau + Li_2(x_\tau^2) + \\ &+ Li_2\left(1 - \frac{x_\tau}{\sqrt{r_\tau}}\right) + Li_2(1 - x_\tau\sqrt{r_\tau}) - \log x_\tau \log\frac{M_\gamma^2}{m_\tau M_\pi}\Bigg].\end{aligned} \tag{B.22}$$

References

[1] J. Gasser and H. Leutwyler, *Chiral perturbation theory to one loop*, *Ann. Phys. (NY)* **158** (1984) 142; *Chiral perturbation theory: expansions in the mass of the strange quark*, *Nucl. Phys.* **B 250** (1985) 465.

[2] G. Ecker, J. Gasser, A. Pich and E. de Rafael, *The role of resonances in chiral perturbation theory*, *Nucl. Phys.* **B 321** (1989) 311.

[3] F. Guerrero and A. Pich, *Effective field theory description of the pion form factor*, *Phys. Lett.* **B 412** (1997) 382 [hep-ph/9707347].

[4] D. Gómez Dumm, A. Pich and J. Portoles, *The hadronic off-shell width of meson resonances*, *Phys. Rev.* **D 62** (2000) 054014 [hep-ph/0003320];
J.A. Oller, E. Oset and J.E. Palomar, *Pion and kaon vector form factors*, *Phys. Rev.* **D 63** (2001) 114009 [hep-ph/0011096].

[5] K. Huber and H. Neufeld, *The decay $\rho^0 \to \pi^+\pi^-\gamma$ and the chiral invariant interactions of vector mesons*, *Phys. Lett.* **B 357** (1995) 221 [hep-ph/9506257].

[6] G. Ecker and R. Unterdorfer, *Four-pion production in e^+e^- annihilation*, hep-ph/0203075.

[7] R. Urech, *Virtual photons in chiral perturbation theory*, *Nucl. Phys.* **B 433** (1995) 234 [hep-ph/9405341].

[8] H. Neufeld and H. Rupertsberger, *Isospin breaking in chiral perturbation theory and the decays $\eta \to \pi l\nu$ and $\tau \to \eta\pi\nu$*, *Z. Physik* **C 68** (1995) 91; *The electromagnetic interaction in chiral perturbation theory*, *Z. Physik* **C 71** (1996) 131 [hep-ph/9506448].

[9] M. Knecht, H. Neufeld, H. Rupertsberger and P. Talavera, *Chiral perturbation theory with virtual photons and leptons*, *Eur. Phys. J.* **C 12** (2000) 469 [hep-ph/9909284].

[10] V. Cirigliano, G. Ecker and H. Neufeld, *Isospin violation and the magnetic moment of the muon*, *Phys. Lett.* **B 513** (2001) 361 [hep-ph/0104267].

[11] ALEPH collaboration, R. Barate et al., *Measurement of the spectral functions of vector current hadronic tau decays*, *Z. Physik* **C 76** (1997) 15; *Measurement of the spectral functions of axial-vector hadronic tau decays and determination of $\alpha_s(M_\tau^2)$*, *Eur. Phys. J.* **C 4** (1998) 409.

[12] J. Bijnens, G. Ecker and J. Gasser, *Radiative semileptonic kaon decays*, *Nucl. Phys.* **B 396** (1993) 81 [hep-ph/9209261].

[13] F.E. Low, *Bremsstrahlung of very low-energy quanta in elementary particle collisions*, *Phys. Rev.* **110** (1958) 974.

[14] J. Wess and B. Zumino, *Consequences of anomalous Ward identities*, *Phys. Lett.* **B 37** (1971) 95;
E. Witten, *Global aspects of current algebra*, *Nucl. Phys.* **B 223** (1983) 422.

[15] J.H. Kühn and A. Santamaria, *Tau decays to pions*, *Z. Physik* **C 48** (1990) 445.

[16] R. Alemany, M. Davier and A. Höcker, *Improved determination of the hadronic contribution to the muon $(g-2)$ and to $\alpha(M_z^2)$ using new data from hadronic τ decays*, *Eur. Phys. J.* **C 2** (1998) 123 [hep-ph/9703220];
M. Davier and A. Höcker, *New results on the hadronic contributions to $\alpha(M_z^2)$ and to $(g-2)_\mu$*, *Phys. Lett.* **B 435** (1998) 427 [hep-ph/9805470];
A. Höcker, *Hadronic contribution to $(g-2)_\mu$*, hep-ph/0111243.

[17] M. Davier and A. Höcker, analysis in preparation.

[18] E. Barberio and Z. Wąs, *Photos: a universal Monte Carlo for QED radiative corrections. Version 2.0*, *Comput. Phys. Commun.* **79** (1994) 291.

[19] W.J. Marciano and A. Sirlin, *Electroweak radiative corrections to tau decay*, *Phys. Rev. Lett.* **61** (1988) 1815; *ibid.* **71** (1993) 3629.

[20] M. Gourdin and E. De Rafael, *Hadronic contributions to the muon g-factor*, *Nucl. Phys.* **B 10** (1969) 667.

[21] S. Narison, *Muon and tau anomalies updated*, *Phys. Lett.* **B 513** (2001) 53 [hep-ph/0103199].

[22] R. Urech, *$\rho^0-\omega$ mixing in chiral perturbation theory*, *Phys. Lett.* **B 355** (1995) 308 [hep-ph/9504238].

[23] CMD-2 collaboration, R.R. Akhmetshin et al., *Measurement of $e^+e^- \to \pi^+\pi^-$ cross section with CMD-2 around ρ-meson*, *Phys. Lett.* **B 527** (2002) 161 [hep-ex/0112031].

[24] J. Portolés, talk given at *QCD 02*, Montpellier, July 2002, to appear in the Proceedings.

[25] J. Bijnens and P. Gosdzinsky, *Electromagnetic contributions to vector meson masses and mixings*, *Phys. Lett.* **B 388** (1996) 203 [hep-ph/9607462].

[26] Particle Data Group (D.E. Groom et al.), *Review of particle physics. Particle data group*, *Eur. Phys. J.* **C 15** (2000) 1.

[27] P. Singer, *Radiative rho-meson decay*, *Phys. Rev.* **130** (1963) 2441, erratum *ibid.* **161** (1967) 1694.

[28] V. Cirigliano, M. Knecht, H. Neufeld, H. Rupertsberger and P. Talavera, *Radiative corrections to K_{l3} decays*, *Eur. Phys. J.* **C 23** (2002) 121 [hep-ph/0110153].

[29] G. Ecker, J. Gasser, H. Leutwyler, A. Pich and E. de Rafael, *Chiral lagrangians for massive spin 1 fields*, *Phys. Lett.* **B 223** (1989) 425.